Agricultural Water Management 128 (2013) 140–148

Contents lists available at SciVerse ScienceDirect

Agricultural Water Management

journal homepage: www.elsevier.com/locate/agwat

# Characteristics of the water–energy–carbon fluxes of irrigated pear (*Pyrus bretschneideri Rehd*) orchards in the North China Plain

Yucui Zhang[a,b], Yanjun Shen[a,*], Xianli Xu[c,d], Hongyong Sun[a], Fang Li[a,b], Qian Wang[a,b]

[a] Key Laboratory of Agricultural Water Resources, Center for Agricultural Resources Research, Institute of Genetics and Developmental Biology, Chinese Academy of Sciences, Shijiazhuang 050021, China
[b] University of Chinese Academy of Sciences, Beijing 100049, China
[c] Key Laboratory for Agro-ecological Processes in Subtropical Region, Institute of Subtropical Agriculture, Chinese of Academy of Sciences, Changesha 410125, China
[d] Huanjiang Observation and Research Station for Karst Ecosystem, Chinese Academy of Sciences, Huanjiang 547100, Guangxi, China

ARTICLE INFO

*Article history:*
Received 30 January 2013
Accepted 9 July 2013

*Keywords:*
Pear
Evapotranspiration
Energy flux
Carbon dioxide

ABSTRACT

Pear trees (*Pyrus bretschneideri Rehd*) play an important role in the fruit production in the North China Plain (NCP) where water shortage is a serious problem. The objectives of this research were to explore the characteristics of water balance, energy transfer and carbon exchange of irrigated pear orchards by a combination of multiple measurement methods (eddy covariance system, sap flow method, and the other equipment). Experiments from 08/01/2011 to 10/31/2012 were conducted in a pear orchard located in the NCP. Annual net radiation (Rn) was 2490 MJ $m^{-2}$ of which latent heat flux accounted for 74.5%, a little higher than the agro-ecosystem with wheat–maize rotation (70%). Annual mean water use efficient (*WUE*) was 1.98 g $CO_2$/kg $H_2O$ which was lower than the agro-ecosystem in the same area. Annual evapotranspiration (*ET*) was 759 mm and daily transpiration (*T*) ranged from 0.5 to 4.3 mm during May to October while daily *T*/*ET* varied from 0.6 to 0.9. Variation of *ET* can be explained well by the change of LAI. As annual drainage was 86 mm, it will take a long time for the shallow soil water (0–140 cm) to replenish deep groundwater. Optimal values of daily downward short wave radiation (Rs) (20 MJ $m^{-2}$ $d^{-1}$) and *ET* (~4.8 mm $d^{-1}$) were probably important thresholds for the plant growth. Changing irrigation method and crops planting structure adjusting according to the water balance and trees growth characteristics, were probably useful for keeping high yield with less water depletion while further research should be done in future.



## 1. Introduction

North China Plain is a very important agricultural region in China, but faces serious water shortage problem (Hu et al., 2010; Liu and Xia, 2004; Shen et al., 2002). Approximately 70% of the plain (~12,600 thousands ha) was irrigated, and the irrigation consumed ~70% of the total water supply (Liu et al., 2001). Irrigation water was mainly extracted from groundwater, large water deficits even led to ground collapse in the NCP (Yang et al., 2006). A study in Hebei province, located in NCP, showed that the decline rate of water table depth reached ~0.7 m $yr^{-1}$ because ~75% of the total irrigated land was irrigated by groundwater in most cropland of this province (Sun et al., 2010). Efficient water use has become very desirable due to the insufficient water availability and the corresponding threats to stable agricultural output (Kang et al., 2003b).

Fruit trees play an important role in the agricultural economic development. Area of orchards in China increased for more than six times during 1982–2007 (China Statistical Yearbook, 2008). Fruit production in the NCP accounted for 22% of the country, and the plant area increased from $4.7 \times 10^5$ to $18.6 \times 10^5$ ha during the past 30 years (1978–2007) (China Rural Statistical Yearbook, 2008). Irrigation is necessary for the fruit trees growth. Area of irrigated orchards in the NCP accounts for 22% of the country (China Rural Statistical Yearbook, 2008). Compared to the herbaceous plant, fruit trees was perennial with deep, developed and low-density root system and easy to absorb deep soil water. Therefore, fruit trees have more potential in the water saving research.

However, it is still difficult to directly measure the evapotranspiration (*ET*) and separately measure evaporation (*E*) and transpiration (*T*) for adult fruit trees with well-developed root system (de Azevedo et al., 2003). With the development of eddy covariance and sap flow methods, the combination of these two approaches was more and more frequently used in the indirect measurement of fruit water depletion research (Liu et al., 2012; Paço et al., 2006; Vandegehuchte et al., 2012; Zhang et al.,

* Corresponding author. Tel.: +86 311 85825464; fax: +86 311 85872248.
*E-mail addresses:* yjshen@sjziam.ac.cn, yj.shen@gmail.com (Y. Shen).

0378-3774/$ – see front matter © 2013 Elsevier B.V. All rights reserved.
http://dx.doi.org/10.1016/j.agwat.2013.07.007

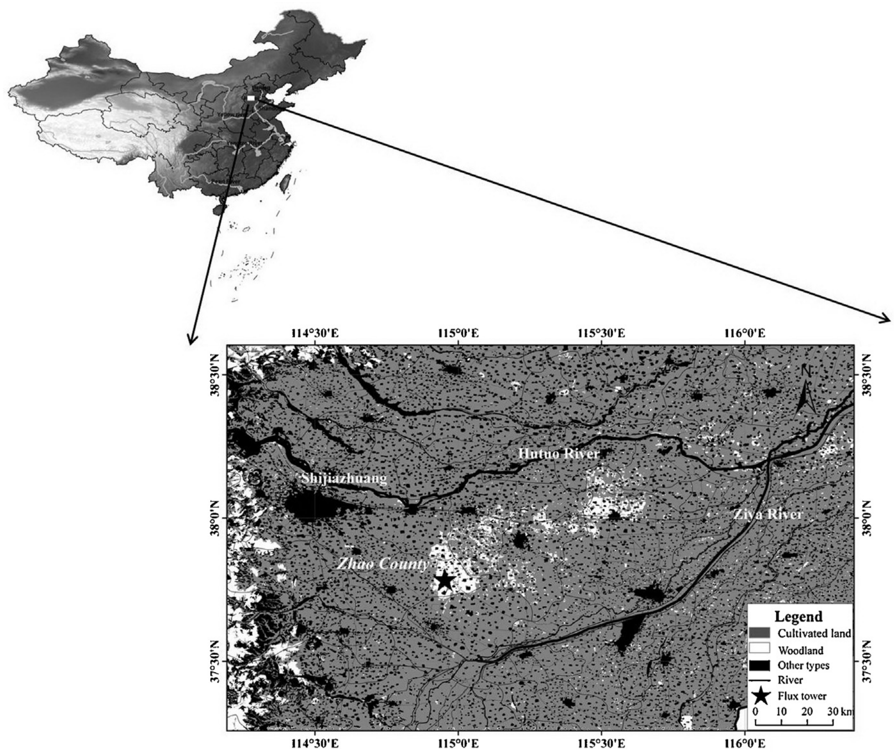


**Fig. 1.** Location and main land use type of the study area.

2011a). At the same time, the water depletion could successfully be partitioned into transpiration and evaporation. For example, transpiration ranged from 1.2 mm to 2.1 mm $d^{-1}$ in an olive orchard during the midseason phonological period while *ET* changed from 1.9 mm $d^{-1}$ to 2.5 mm $d^{-1}$ (Cammalleri et al., 2012). Nonetheless, little research focuses on the water consumption of fruit trees growing in the semi-arid and semi-humid area, especially in the water shortage region with deep water table depth and large irrigation withdrawal.

Even some studies have already paid much attention on fruit trees such as olive, mango, vineyards and apple, few concerns on pears (Yunusa et al., 2004; Teixeira et al., 2008; Zhang et al., 2007; Liu et al., 2012). However, pear plays critical role in fruit planting with its coverage approximately 10% of the total fruit planting area in China. Pear exports and yields of China accounted for approximately 20% (2003) and 63% (2007) of the world (FAO database: http://faostat.fao.org/), respectively. Pear production in the NCP accounts for 40% of the country (China Rural Statistical Yearbook, 2009). There is a continuous pressure for improvements in water use efficient in irrigated pear orchards in the NCP.

Therefore, the main objectives of the paper were to (1) explore the characteristics and relationships of water, energy and carbon dioxide fluxes for pear trees, and also compare it with agro-ecosystem (winter wheat–summer maize); and (2) partition evapotranspiration into *T* and *E* for pear trees.

## 2. Materials and methods

### 2.1. Site descriptions

We conducted our experiments in Hebei province, an important agriculture production area in NCP. Pear cultivation accounted for 20% of the total orchard area and 3% of the total farmland in Hebei Province (China Rural Statistic Book, 2011). Yield of pear accounted for almost 40% of the total fruit production. Meanwhile, huge amount of water was used for the orchards irrigation. The irrigated orchard area was 296 thousand ha in Hebei Province, which accounted for approximately 24% of the total area of the whole country (China Statistical Yearbook, 2010).

The experimental location, (Zhao County of Hebei province as shown in Fig. 1), is cultivated with pear orchard (*Pyrus bretschneideri Rehd*) (37°47′44″ N, 114°55′57″ E, and altitude of 40 m) ~40 km from Shijiazhuang City, Hebei Province, China. The cultivated area of pear trees in Zhao County can reach 16,700 ha and the yield was $3.8 \times 10^8$ kg $yr^{-1}$. This area has a semi-arid monsoonal climate. The mean annual temperature is 12.3 °C with the mean annual sunshine hour 2751.2 h, and the annual accumulated temperature (>0 °C) is 4768.6 °C. The annual precipitation is ~503 mm (Gao et al., 2012). Water table depth in this area decreased from 46 m to 50 m from Jul., 2011 to Jul., 2012. The experiment was conducted from 1st Aug. 2011 to 31st Oct. 2012. However, the water balance equation was calculated by the data from 1st Oct., 2011 to 30th Sep., 2012 and the other annual values mentioned in this study were also calculated by the data in the same periods.

The pear trees were planted in 1988 with an average height of 5.0 m, and an interval of 5.0 m between rows by 4.0 m between trees. Each tree was about 24 years old with a trunk diameter between 180 and 250 mm and had been pruned as a central leader. The orchard was managed according to local commercial practices for fertilization, pest management, weed control, and winter pruning. Fruit thinning was applied in 15–20 days after flower drop. Fruit spacing was 15–25 cm. The phenological stages were divided into the following: sprouting (Mar.), blooming (Apr.), fruit formation (May–August), fruit maturation (Sep.) and leaves abscission (Oct.). The orchard was flood-irrigated (70 mm once) between the rows and the annual irrigation was 420 mm.

The soil mainly consists of silty loam at the depth of 0–100 cm and clay loam below 100 cm and was suitable for the pear trees growth. The soil organic matter content and the other composition of soil nutrient were shown in Table 1. Soil moisture field capacity

**Table 1**
The soil organic matter content and the other composition of soil nutrient.

| Soil organic matter, % | Available | | | | | PH |
|---|---|---|---|---|---|---|
| | Nitrogen, mg/kg | Phosphate, mg/kg | Potassium, mg/kg | Iron, mg/kg | Zinc, mg/kg | |
| 0.8 | 26.2 | 41.7 | 104.2 | 5.3 | 0.6 | 8.2 |

is approximately 35% above 100 cm. The viable roots were mainly distributed in 0–100 cm soil layer.

### 2.2. Experimental design and measurements

The experimental site covers ~2664 $m^2$, and the area of the total orchard is ~5.2 $km^2$. Three replicate trees were randomly selected for the sap flow measurements. These three trees were located in the prevailing direction of the wind near the flux tower (Fig. 2). Soil samples collected for the soil organic matter and nutrient content measurement analysis were from different directions of the orchards with five replicates (Fig. 2). The soil moisture ($\theta$) was hourly recorded by $ECH_2O$ system (Decagon, USA) at five depths (10, 30, 50, 80, and 120 cm) and averaged every 5 days. A soil pit was dug between two trees and sensors were inserted at an angle of 45° in order to protect the connection and have a close conjunction between sensors and soil. Water table depth was measured by the water level logger (Hobo U20-001-01, Onset Corp., Bourne, MA). Leaf area index (LAI) was acquired from the MODIS production (1 km, MOD15A2). The accuracy of the LAI data was low, so just the change trend was mainly analyzed. Precipitation (*P*), air temperature (Ta) and relative humidity (Rh) were collected in the local meteorological agency, which was about 13 km distance from the experimental plots. The compared water and energy fluxes data of crops were from Luancheng experimental station, which was about 20 km from this pear orchard under similar climate conditions (Shen et al., 2013).

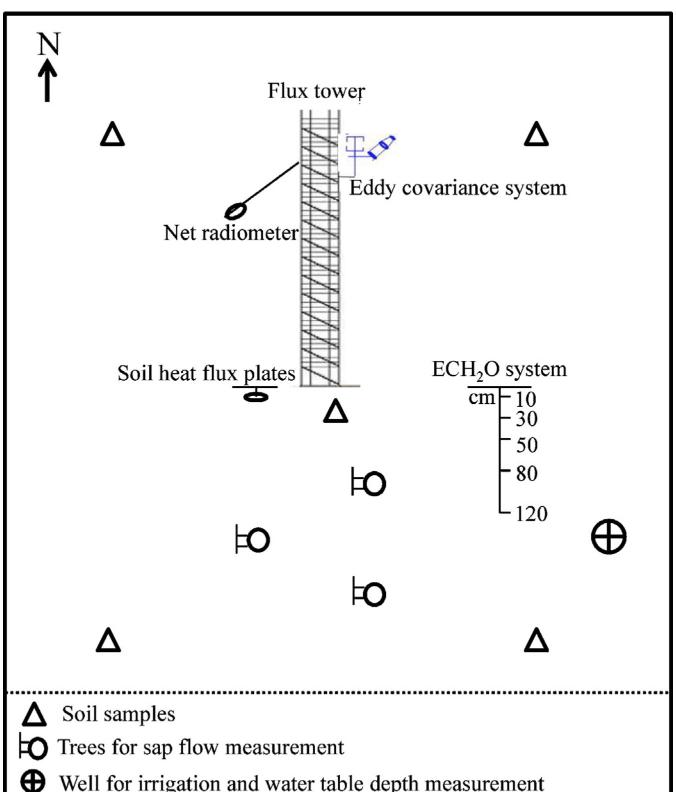


**Fig. 2.** Field experiment sketch in the pear orchard.

### 2.3. Water and energy fluxes observation and calculation

The energy flux contains latent heat (LE), sensible heat (Hs), net radiation (Rn), and soil heat flux (*G*). The eddy covariance system installed at 7.5 m was used to determine LE (MJ $m^{-2}$ $d^{-1}$) and Hs (MJ $m^{-2}$ $d^{-1}$) by a three-axis sonic anemometer (CSAT3, Campbell Scientific, Logan, UT, USA) and LI7500 $H_2O/CO_2$ gas analyzer (LI-COR, Inc., Lincoln, NE, USA) (Fig. 2). The research area had a good fetch (>800 m) and uniform underlying surface (pear trees). Net radiation (Rn, MJ $m^{-2}$ $d^{-1}$) was monitored with a CNR-1 net radiometer (Kipp & Zonen) and soil heat flux (*G*, MJ $m^{-2}$ $d^{-1}$) was monitored using two soil heat flux plates (HFP01SC, Hukseflux), buried at a depth of 2 cm beneath the soil surface. All these equipment were connected to a CR3000 data logger (Campbell Scientific, Logan, UT, USA) and were calculated in the frequency of half-hour data. The three dimensional wind velocity, vapor, and $CO_2$ concentrations were sampled at a frequency of 10 Hz. Monitoring results were averaged in 30 min intervals and processed with Eddypro (LI-COR, http://www.licor.com/env/products/eddy_covariance) which includes the coordinate rotation of the 3D sonic wind speed vectors (Wilczak et al., 2001), Webb, Pearman & Leuning correction (Webb et al., 1980), night flux correction (Gu et al., 2005; Saleska et al., 2003; Zhu et al., 2006) and the data quality control (Mauder et al., 2006; Yu et al., 2006). For the missing flux data, the mean diurnal variation method was applied using a 7-day data window (Falge et al., 2001). The daily energy values were calculated by the 24-hour data. Evapotranspiration was calculated by LE and the latent heat of vaporization of water. The Bowen ratio ($\beta$) is estimated from measurements of Hs and LE. Net ecosystem exchange for $CO_2$ (*NEE*, g C $m^{-2}$ $day^{-1}$) was converted from the carbon dioxide flux (*Fc*, g $CO_2$ $m^{-2}$ $day^{-1}$). And the water use efficiency (*WUE*, g $CO_2$/kg $H_2O$) was calculated by:

$$WUE = \frac{Fc}{ET} \quad (1)$$

Soil water drainage (*D*, mm) was calculated using a water balance equation:

$$D = P + I - ET - \Delta W \quad (2)$$

where *P* is precipitation (mm); *I* is irrigation applications (mm), *ET* is evapotranspiration (mm), and $\Delta W$ is soil water depletion in the measured soil depth range (0–140 cm). Soil water depletion was calculated from the soil moisture ($\theta$). Runoff was ignored because there is usually no runoff in pear orchards of the NCP.

Sap flow was measured by TDP (Thermal Dissipation Probe, TDP30-FLGS-TDP XM1000, Dynamax, USA) based on the liquid velocity heat dissipation theory (Granier, 1985, 1987; Granier et al., 1996), and the data were logged by the data logger CR1000 (Campbell Scientific, Logan, UT, USA). A probe set consisted of two needles, a heated needle above and a reference needle below. The heated needle had a heating element and a copper-constantan thermo junction inserted in a 1.2 mm diameter (o.d.) stainless steel tube that was 30 mm long. The reference needle had no heating element. The probe electronics were sealed with an epoxy resin that was impervious to water. According to the research of Granier (year), the sap flow rate (Fs, $cm^3$/h) was calculated by:

$$Fs = As \times V \times 3600 \quad (3)$$

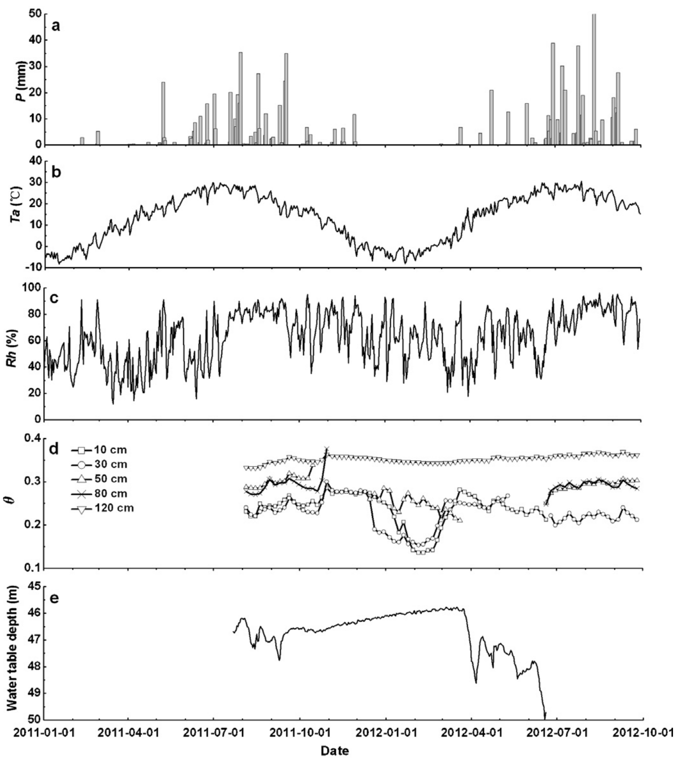


**Fig. 3.** Daily values of weather variables, soil moisture ($\theta$) and water table depth during 2011 to 2012 in Zhao County ($P$: precipitation; Ta: air temperature; Rh: relative humidity).

where *As* was the crossing-sectional area of sap conducting wood ($cm^2$); $V$ was the average sap flow velocity (cm/s). The sapwood area was calculated by the heartwood area subtracting from trunk cross-sectional area. Trees were cut in the orchard adjacent to the plots in Dec. 2011 with the same growth conditions and management measures, in which ten trees were selected to measure this cross-sectional area. Average sap flow velocity was calculated by the dimensional parameter $K$:

$$V = 0.0119 \times K^{1231} \tag{4}$$

and

$$K = \frac{dTM - dT}{dT} \tag{5}$$

$dT$ (°C) was the measured difference in temperature between that of heated needle. The value of $dT$ was found from the differential voltage measured between the upper and lower thermocouple. The parameter $dTM$ is the value of $dT$ when there was no sap flow. In this research, dTM equals to 3.23 °C, appeared at 1:00 to 3:00 of the day. Meanwhile, according to the cultivated density of the pear trees (414 trees per hectare, calculated by the row spacing and planted distance), the transpiration was available.

## 3. Results and discussion

### 3.1. Annual variations in weather and orchards environmental variables

The annual precipitation is 507 mm (Fig. 3a), most of which occurs from June to September accounting for approximately 82% of the total amount. The maximum of temperature also appears during June to September (30.5 °C). Precipitation and energy flux are over the same period which is favorable for the pear trees growth. The annual mean temperature is 12.9 °C (Fig. 3b) and the relative humidity is 67% (Fig. 3c), which are almost the same as the agro-ecosystem in this area ($T$: 12.6 °C and Rh: 71% in the same periods). Soil moisture changes along with the precipitation and irrigation while it is stable when the depth reaches 120 cm (Fig. 3d). The average soil water content is 0.24, 0.23, 0.28, 0.29 and 0.35 for the depth of 10, 30, 50, 80 and 120 cm, respectively. The annual average $\theta$ of orchard and cropland is also same as each other. Water table depth decreased from 48 m to 51 m during 20th Jul. 2011 to 20th Jun. 2012 and it decreased obviously when there were irrigations in Mar., Apr., May, Jun., and Oct. (Fig. 3e) while minor increments occurred immediately after the rainy season, which is a common phenomenon in the North China Plain.

### 3.2. Annual variations in energy fluxes and net ecosystem exchange of carbon dioxide (NEE)

The energy balance closure ((LE + Hs)/(Rn − $G$)), usually used to evaluate the effectiveness of the eddy covariance system, was ~0.9 in this research which achieved the general level (70–90%). The imbalance is very common in the similar research (Teixeira et al., 2008; Twine et al., 2000) because of the measurement error of the eddy covariance system itself.

Energy and carbon dioxide fluxes have their respective annual and seasonal characteristics. Same as the agro-ecosystem in the NCP (Shen et al., 2013), Rn has a parabola-like change with an obvious peak (Fig. 4a). The maximum of Rn is 19.0 MJ $m^{-2}$ $d^{-1}$ appears in June while the minimum is −0.8 MJ $m^{-2}$ $d^{-1}$ in December and annual Rn was 2490 MJ $m^{-2}$. The sensible heat flux of pear orchard is very different from the agro-ecosystem (wheat–maize rotation) in the same area. There is only one peak ~5.2 MJ $m^{-2}$ $d^{-1}$ appeared in March (Fig. 4b) in pear orchard, but there always appears two peaks in April and July for the wheat–maize rotation field in the NCP. Change trend of LE is similar to Rn, with the maximum value of ~18.0 MJ $m^{-2}$ $d^{-1}$ in June (Fig. 4c). Annual LE accounted for 75% of Rn which is a little higher than the agro-ecosystem (70%) in the NCP (Zhang et al., 2002) while Hs/Rn is 16%. Soil heat flux always keeps low like the agro-ecosystem, and the annual accumulation of $G$ is −8 MJ $m^{-2}$ (Fig. 4d). It is always higher in the trees growing periods and lower in winter. Bowen ratio (Fig. 4e) can reflect the partition of Rn between LE and Hs and it is also influenced by soil moisture. The maximum value of $\beta$ appears in January to February with low evapotranspiration and soil moisture (Fig. 4e and Fig. 2d, 2012).

The negative net ecosystem exchange of $CO_2$ indicates a $CO_2$ sequestration by pear orchard whereas positive *NEE* values represent a $CO_2$ source. Annual *NEE* could reach ~−600 g C $m^{-2}$, and (absolute value) is lower than the agro-ecosystem of −760 g C $m^{-2}$. There is only one peak (−7.7 g C $m^{-2}$ $d^{-1}$, Fig. 4f) during the vigorous growth period between May and September while the winter wheat–summer maize agro-ecosystem has two obvious peaks in the NCP (Shen et al., 2013). However, the *NEE* for pear trees keeps relative high sequestration capability (−3.0 to −7.7 g C $m^{-2}$ $d^{-1}$) from May to October, not like for the agro-ecosystem that just has high capability in May and August. The different carbon exchange characteristics are probably caused by the difference of phenology between the pear trees and crops.

In order to figure out the daily differences of energy and carbon dioxide exchange during growth periods, several typical sunny days were selected for a further study (Fig. 5). These selected six typical sunny days stand for earlier sprouting (Fig. 5a), flowering (Fig. 5b), fruit formation (Fig. 5c–e), and fruit maturation stages (Fig. 5f), respectively. The Rn of all these days showed an inverted ‘V’ type with the peak value about 300–400 W $m^{-2}$ at 12:00, and it turned to negative value before 6:00 and after 18:00. The daily variation of LE for these days is consistent with Rn while they have different

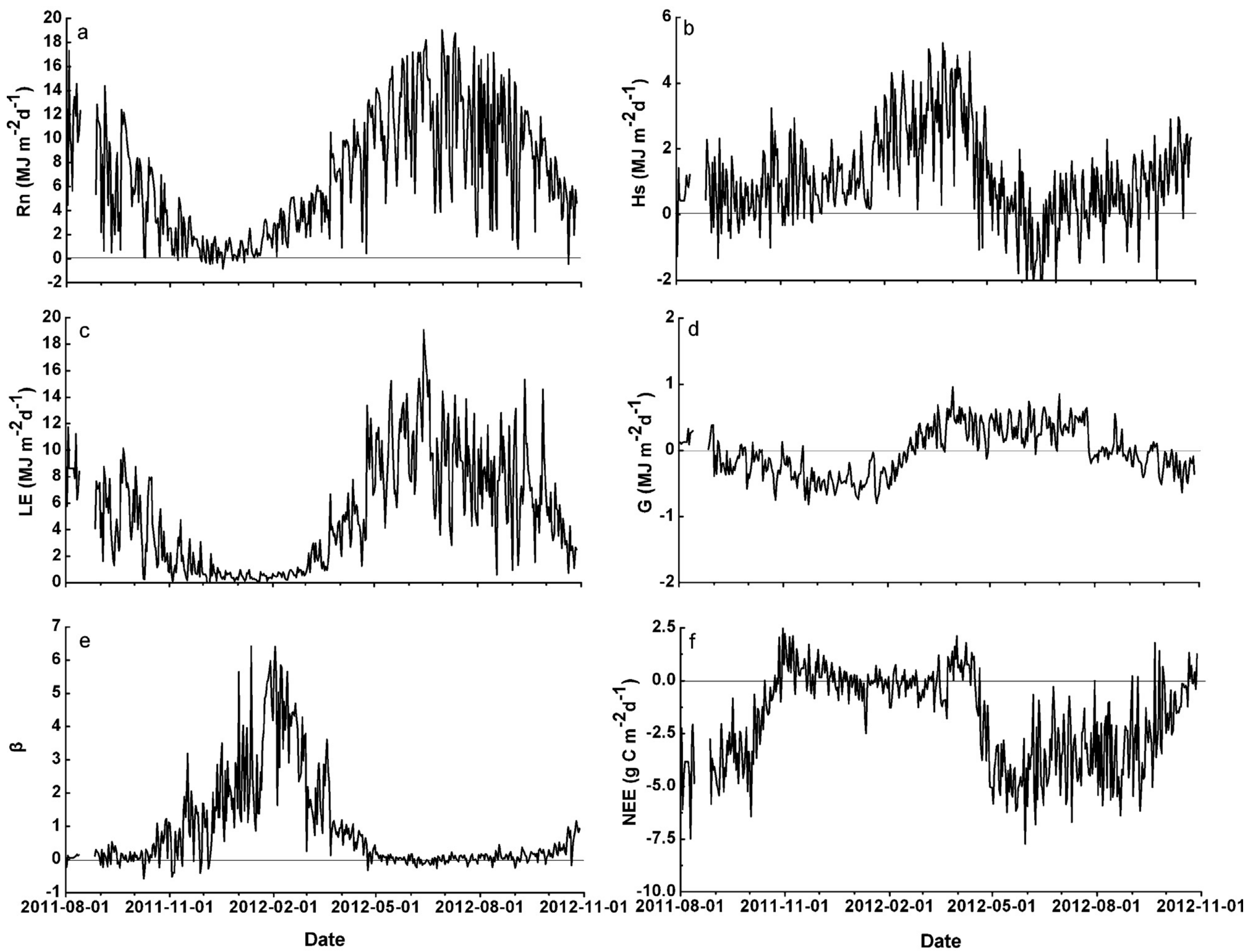


**Fig. 4.** Annual variations in daily net radiation (Rn), latent heat flux (LE), sensible heat flux (Hs), soil heat flux (*G*), Bowen ratio ($\beta$) and net ecosystem exchange of carbon dioxide (NEE) in the pear orchards in the North China Plain.

values. All of the peak values for the daily energy flux appeared during 10:00–14:00. Maximum daily latent heat flux increases from 20 W $m^{-2}$ in earlier sprouting (06/05/2012) to 340 W $m^{-2}$ in fruit formation stage and then declines to 200 W $m^{-2}$ in fruit maturation stage. Sensible heat fluxes become smaller when LE is larger. Soil heat fluxes keep low (<20 W $m^{-2}$) in earlier sprouting and fruit maturation stages, and it keeps ~60 W $m^{-2}$ in the other growth periods except for 06/05/2012 because of the high soil moisture caused by the 16 mm precipitation in 06/02/2012. The carbon dioxide flux keeps a high value (−1.0 to −1.5 mg $CO_2$ $m^{-2}$ $s^{-1}$) at 10:00 to 14:00 during the fruit formation stage which is also the rapid growth periods. Because the photosynthesis is much stronger during the daytime in this period (fruit formation stage) than in February and the end of September, there was not obvious closure of stomata during midday for this pear variety (*P. bretschneideri Rehd*) like winter wheat in the NCP (Baldocchi, 1994; Wang et al., 2006).

### 3.3. Evapotranspiration partition, water use efficiency (WUE) and water balance for the pear orchards

Seasonal pattern of evapotranspiration (*ET*) for pear trees is also different from that of the wheat–maize crop system (Fig. 6a). There is only one peak in a year and the maximum is ~8 mm $d^{-1}$ for pear trees. The annual *ET* of pear trees was 759 mm which is 1.1 times of the agro-ecosystem, and this result is comparable to the similar research (657 mm, 36°35′ N, 114°30′ E; Cheng et al., 2012; 865 mm, 40°26′ S, 145°16′ E, Kang et al., 2003a). Evapotranspiration increased since April after flowering and decreased until very low after the fruit harvest. By the sap flow measurement since 28th Apr. 2012, the evapotranspiration was partitioned into transpiration and evaporation. Daily transpiration ranged from 0.5 to 4.3 mm during May to October and had good linear relationship with *ET* ($R^2$ = 0.8). However, the ratio *T*/*ET* did not change a lot during the same period, which varied from 0.6 to 0.9 (mean value: 0.77). This phenomenon implied that transpiration determined the change of *ET* from May to October for pear orchard. Although *ET* also determined by transpiration, value of *T*/*ET* in milking period for winter wheat in the NCP was ~0.87 (Zhang et al., 2011b), a little higher than the pear trees in the vigorous growth periods (May to October). However, this high *T*/*ET* of agro-ecosystem does not last as long as the pear orchards, therefore, the annual water consumption (*ET*) of agro-ecosystem is less. Water use efficiency (Fig. 6b) was higher in May and September than the other months. Because *ET* of the pear trees was not very high in these periods and *Fc* was relatively high. The average *WUE* from April to September in 2012 was 3.80 g $CO_2$/kg $H_2O$, and the annual mean *WUE* was 1.98 g $CO_2$/kg $H_2O$ which was lower than the agro-ecosystem (4.00 g $CO_2$/kg $H_2O$) in the same area (Fang et al., 2010; Sun et al., 2010; Shen et al., 2013). Because the leaf area index (LAI) data were achieved from MODIS product, the precision should be lower than measurement. However, the changing trend was valuable for reference. About 75% ($R^2$ of *ET* and LAI) variation of *ET* can be explained by the change of LAI (Fig. 7). Leaf area index increased quickly after the earlier sprouting, and began to decrease at the

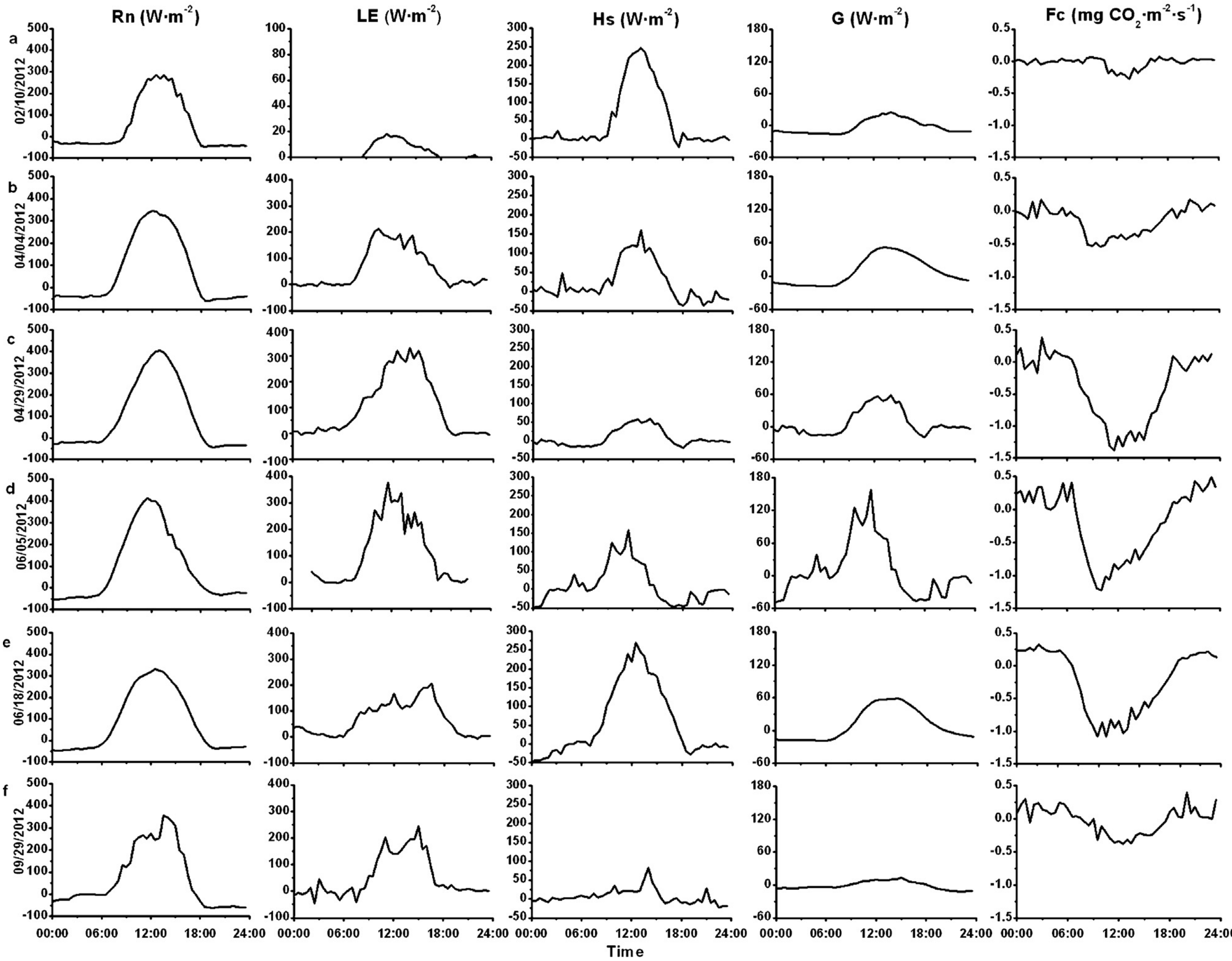


**Fig. 5.** Energy (Rn: net radiation; LE; latent heat flux; *H*: sensible heat flux; *G*: soil heat flux) and carbon dioxide fluxes (*Fc*) variation in different growth periods (a: earlier sprouting; b: blooming; c–e: fruit formation; f: fruit maturation).

beginning of June while the maximum of LAI (3.0) also appeared in June.

Based on the balance of evapotranspiration, precipitation, irrigation, and soil water depletion, the monthly and annual drainage of the pear orchard was calculated (Table 2). There were 10 out of the 12 months with drainage to the deep soil ranging from 1 to 53 mm/month because of irrigation and precipitation. The annual drainage was 86 mm, which is much larger than the 31 mm $yr^{-1}$ of the agro-ecosystem (Sun et al., 2010) because of the silty soil texture from 0 to 100 cm of our experiment site. As the ground water table (50.8 m) declined at the speed of 0.7 m $yr^{-1}$ in this area, it will take a long time for the deep groundwater receiving the replenishment of shallow soil water (0–140 cm).

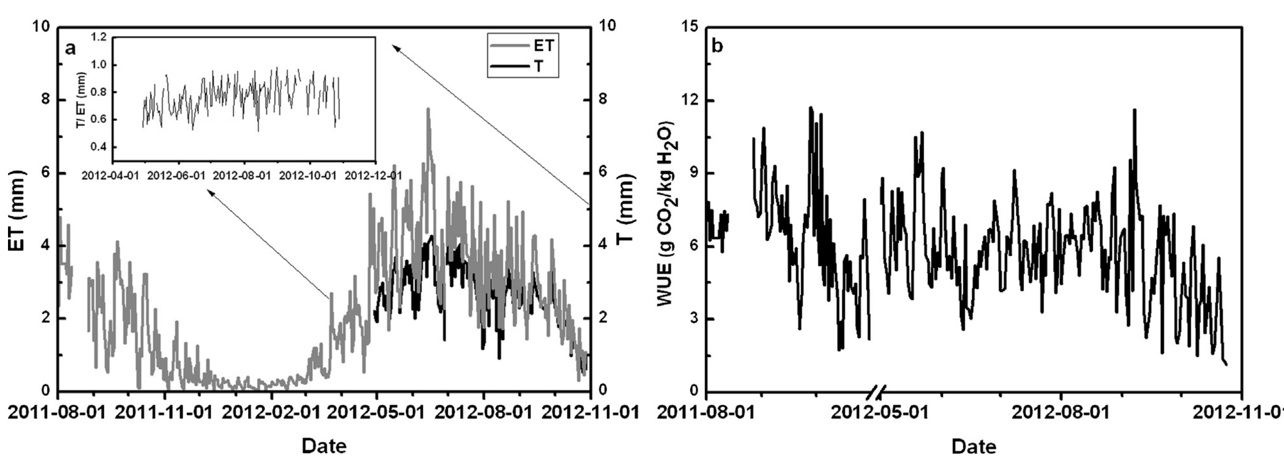


**Fig. 6.** Evapotranspiration (*ET*) and its partition (T: transpiration) and the annual variation of water use efficiency (*WUE*).

**Table 2**
Annual and monthly water balance for the pear orchards (*P*: precipitation; *ET*: evapotranspiration; Δ*W*: soil water depletion; *I*: irrigation; *D*: drainage) in the North China Plain.

| Date | *P* (mm) | *ET* (mm) | Δ*W* (mm) | *I* (mm) | *D* (mm) |
|---|---|---|---|---|---|
| Annual | **507** | **759** | **82** | **420** | **86** |
| 10/2011 | 15 | 49 | 34 | 70 | 2 |
| 11/2011 | 30 | 18 | 12 | 0 | 1 |
| 12/2011 | 0 | 8 | −12 | 0 | 3 |
| 01/2012 | 0 | 5 | −9 | 0 | 3 |
| 02/2012 | 0 | 8 | 16 | 0 | −24 |
| 03/2012 | 8 | 31 | 22 | 70 | 25 |
| 04/2012 | 26 | 68 | 19 | 70 | 8 |
| 05/2012 | 14 | 127 | −38 | 70 | −5 |
| 06/2012 | 92 | 133 | 24 | 70 | 5 |
| 07/2012 | 144 | 123 | 20 | 0 | 2 |
| 08/2012 | 89 | 100 | −24 | 0 | 13 |
| 09/2012 | 89 | 89 | 18 | 70 | 53 |

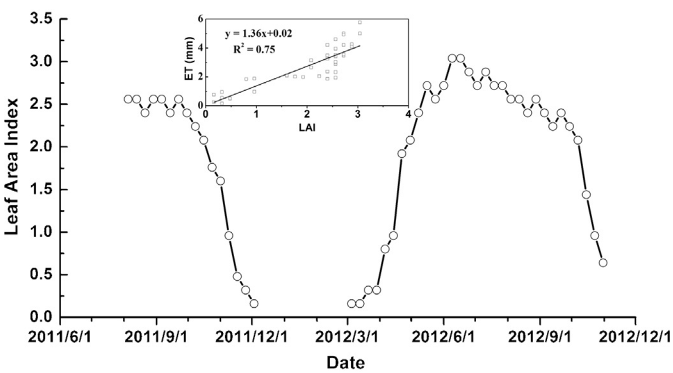


**Fig. 7.** Leaf area index (LAI) change trend from Aug. 2011 to Oct. 2012 and its relationship with evapotranspiration (*ET*).

Table 2 shows that evapotranspiration exceeds precipitation in Mar., Apr., May, Jun. and Oct., and this suggests that the first four months are the key periods for water requirement. Therefore, timely irrigation was conducted in these months in order to keep high yield. In August, *ET* is also higher than precipitation and soil water covers the shortage while orchard is irrigated at the beginning of next month. Water deficits happen in winter except in Feb. with the enough melt water. However, this deficit will not affect the pear trees growth significantly. Monthly water balance analysis shows that more irrigation should be practiced in May while irrigation in Sep. and Oct. should be reduced. Orchards irrigated as the calculated reference evapotranspiration was more reasonable than flood irrigation. According to the trees growth characteristics, deficit irrigation also was worth trying (Marsal et al., 2002, 2012; Kang et al., 2003a,b), which will probably save more water than the flood irrigation and keep high yield.

### *3.4. Influences of water and energy fluxes on net ecosystem exchange of $CO_2$*

Net ecosystem exchanges of $CO_2$ determined the yield and were strongly influenced by the available radiation and evapotranspiration. In order to describe the relationship conveniently and intuitively, we add a minus before *NEE* (−*NEE*) to analyze the influences of downward short wave radiation (Rs) and *ET* (Fig. 8). The boundary line was fitted including 90% of the total data. The pear orchard ecosystem become a carbon sink when Rs exceeds the critical value of 2.5 MJ $m^{-2}$ $d^{-1}$ (Fig. 8a). The −*NEE* capacity reaches a plateau of 5.3 g C $m^{-2}$ $d^{-1}$ when the daily mean Rs exceeds 20 MJ $m^{-2}$ $d^{-1}$. On the other hand, −*NEE* is limited by water availability as well (Fig. 8b). Maximum −*NEE* is found when *ET* is ~4.5 mm $d^{-1}$ and then the −*NEE* decreases when *ET* is higher. The thresholds of Rs and *ET* are similar to the winter wheat (the corresponding values were 18 MJ $m^{-2}$ $d^{-1}$ and 4 mm $d^{-1}$) in the NCP (Shen et al., 2013). Therefore, carbon accumulation depends on not only available energy but also suitable water availability.

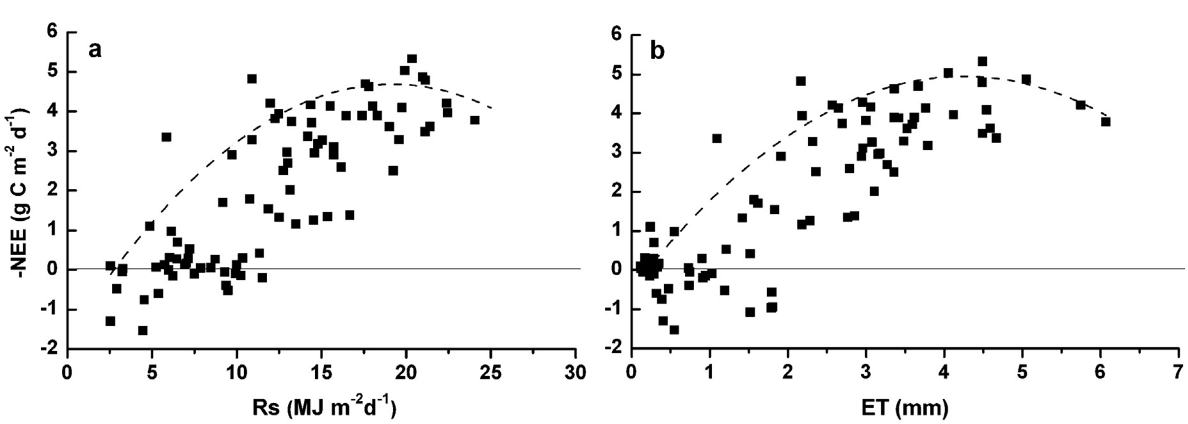


**Fig. 8.** Relationship among negative net ecosystem exchange of $CO_2$ (−*NEE*), downward short wave radiation (Rs), and evapotranspiration (*ET*) (all dots represent 5-day mean values during 08/01/2011 to 10/30/2012).

## 4. Conclusions

Based on the eddy covariance system and sap flow measurement, the water and energy balance and carbon dioxide exchange of pear orchard was analyzed in this research. Annual Rn was 2490 MJ $m^{-2}$; annual LE accounted for 75% of Rn which was a little higher than the agro-ecosystem (70%) in the NCP. There was only one peak for all the fluxes during the annual variation, which is very different from the agro-ecosystem of winter wheat–summer maize rotation in the NCP due to differences in phenological characteristics. Annual *NEE* could reach ∼−600 g C $m^{-2}$, lower than the agro-ecosystem (−760 g C $m^{-2}$). The annual mean *WUE* was 1.98 g $CO_2$/kg $H_2O$ which was lower than the agro-ecosystem (4.00 g $CO_2$/kg $H_2O$) in the same area.

The annual *ET* of pear trees was 759 mm while daily transpiration ranged from 0.5 to 4.3 mm during May to October. The ratio of *T*/*ET* did not change a lot during the same period ranging from 0.6 to 0.9. Variation of *ET* can be explained by the change of LAI. As calculated by the water balance equation, the annual drainage was 86 mm. Monthly water balance analysis shows that more irrigation should be conducted in May while irrigation in Sep. and Oct. should be reduced. However, considering the present water table depth and recharge rate, it will take a long time for the shallow soil water (0–140 cm) to replenish deep groundwater. Pear trees consumed more water per year and had lower *WUE* than agro-ecosystem. Carbon accumulation depended on not only available energy but also available water (for evapotranspiration). In order to get the maximum of (negative) *NEE*, optimal values of daily Rs and *ET* were 20 MJ $m^{-2}$ $d^{-1}$ and ∼4.5 mm $d^{-1}$, respectively, similar to that of the winter wheat in the agro-ecosystem, which means these two values probably be important threshold for the plant growth. Orchards irrigated as the calculated reference evapotranspiration was more reasonable than flood irrigation. According to the trees growth characteristics, deficit irrigation also was worth trying (Marsal et al., 2002, 2012; Kang et al., 2003a,b). These measurements are probably useful for keeping high yield but with less water depletion. Meanwhile, adjusting crops planting structure is also very helpful, such as reducing planting area of pear trees and increasing low water consumption trees or varieties. These two methods need to be tested and verified in the future research.

## Acknowledgments

This research was supported by the knowledge innovation projects of Chinese Academy of Sciences (Nos: KSCX2-EW-J-5 and KZCX2-YW-448). Xianli Xu was supported by “100 talents program” of Chinese Academy of Sciences (Y323025111 and Y251101111).

## References

Baldocchi, D., 1994. A comparative study of mass and energy exchange rates over a closed $C_3$ (wheat) and an open $C_4$ (corn) crop: II. $CO_2$ exchange and water use efficiency. Agricultural and Forest Meteorology 67, 291–321.

Cammalleri, C., Rallo, G., Agnese, C., Ciraolo, G., Minacapilli, M., Provenzano, G., 2012. Combined use of eddy covariance and sap flow techniques for partition of ET fluxes and water stress assessment in an irrigated olive orchard. Agricultural Water Management, http://dx.doi.org/10.1016/j.agwat.2012.10.003.

Cheng, F., Sun, H., Shi, H., Zhao, Z., Wang, Q., Zhang, J., 2012. Effects of regulated deficit irrigation on the vegetative and generative properties of the pear cultivar ‘Yali’. Journal of Agricultural Science and Technology 14, 183–194.

de Azevedo, P.V., da Silva, B.B., da Silva, V.P.R., 2003. Water requirements of irrigated mango orchards in northeast Brazil. Agricultural Water Management 58, 241–254.

Falge, E., Baldocchi, D., Olson, R., Anthoni, P., Aubinet, M., Bernhofer, C., Burba, G., Ceulemans, R., Clement, R., Dolman, H., 2001. Gap filling strategies for defensible annual sums of net ecosystem exchange. Agricultural and Forest Meteorology 107, 43–69.

Fang, Q.X., Ma, L., Green, T.R., Yu, Q., Wang, T.D., Ahuja, L.R., 2010. Water resources and water use efficiency in the North China Plain: current status and agronomic management options. Agricultural Water Management 97, 1102–1116.

Gao, L.X., Guo, Z., Li, P.C., 2012. Production standard of pear (*Pyrus bretschneideri Rehd*) as green food in Zhao County. Hebei Fruit 5, 18–19.

Granier, A., 1985. Une nouvelle méthode pour la mesure du flux de sève brute dans le tronc des arbres. Annals of Forest Science 42, 193–200.

Granier, A., 1987. Evaluation of transpiration in a Douglas-fir stand by means of sap flow measurements. Tree Physiology 3, 309–320.

Granier, A., Huc, R., Barigah, S., 1996. Transpiration of natural rain forest and its dependence on climatic factors. Agricultural and Forest Meteorology 78, 19–29.

Gu, L., Falge, E.M., Boden, T., Baldocchi, D.D., Black, T., Saleska, S.R., Suni, T., Verma, S.B., Vesala, T., Wofsy, S.C., 2005. Objective threshold determination for nighttime eddy flux filtering. Agricultural and Forest Meteorology 128, 179–197.

Hu, Y., Moiwo, J.P., Yang, Y., Han, S., Yang, Y., 2010. Agricultural water-saving and sustainable groundwater management in Shijiazhuang Irrigation District, North China Plain. Journal of Hydrology 393, 219–232.

Kang, S., Hu, X., Du, T., Zhang, J., Jerie, P., 2003a. Transpiration coefficient and ratio of transpiration to evapotranspiration of pear tree (*Pyrus communis* L.) under alternative partial root-zone drying conditions. Hydrological Processes 17, 1165–1176.

Kang, S., Hu, X., Jerie, P., Zhang, J., 2003b. The effects of partial rootzone drying on root, trunk sap flow and water balance in an irrigated pear (*Pyrus communis* L.) orchard. Journal of Hydrology 280, 192–206.

Liu, C., Du, T., Li, F., Kang, S., Li, S., Tong, L., 2012. Trunk sap flow characteristics during two growth stages of apple tree and its relationships with affecting factors in an arid region of northwest China. Agricultural Water Management 104, 193–202.

Liu, C., Xia, J., 2004. Water problems and hydrological research in the Yellow River and the Huai and Hai River basins of China. Hydrological Processes 18, 2197–2210.

Liu, C., Yu, J., Kendy, E., 2001. Groundwater exploitation and its impact on the environment in the North China Plain. Water International 26, 265–272.

Marsal, J., Lopez, G., Mata, M., Girona, J., 2012. Postharvest deficit irrigation in ‘Conference’ pear: effects on subsequent yield and fruit quality. Agricultural Water Management 103, 1–7.

Marsal, J., Mata, M., Arbonés, A., Rufat, J., Girona, J., 2002. Regulated deficit irrigation and rectification of irrigation scheduling in young pear trees: an evaluation based on vegetative and productive response. European Journal of Agronomy 17, 111–122.

Mauder, M., Liebethal, C., Göckede, M., Leps, J.P., Beyrich, F., Foken, T., 2006. Processing and quality control of flux data during LITFASS-2003. Boundary-Layer Meteorology 121, 67–88.

Paço, T., Ferreira, M., Conceiçao, N., 2006. Peach orchard evapotranspiration in a sandy soil: comparison between eddy covariance measurements and estimates by the FAO 56 approach. Agricultural Water Management 85, 305–313.

Saleska, S.R., Miller, S.D., Matross, D.M., Goulden, M.L., Wofsy, S.C., da Rocha, H.R., de Camargo, P.B., Crill, P., Daube, B.C., de Freitas, H.C., 2003. Carbon in Amazon forests: unexpected seasonal fluxes and disturbance-induced losses. Science 302, 1554–1557.

Shen, Y., Kondoh, A., Tang, C., Zhang, Y., Chen, J., Li, W., Sakura, Y., Liu, C., Tanaka, T., Shimada, J., 2002. Measurement and analysis of evapotranspiration and surface conductance of a wheat canopy. Hydrological Processes 16, 2173–2187.

Shen, Y., Zhang, Y., Scanlon, B.R., Lei, H., Yang, D., Yang, F., 2013. Energy/water budgets and productivity of the typical croplands irrigated with groundwater and surface water in North China Plain. Agricultural and Forest Meteorology (in press).

Sun, H., Shen, Y., Yu, Q., Flerchinger, G., Zhang, Y., Liu, C., Zhang, X., 2010. Effect of precipitation change on water balance and WUE of the winter wheat–summer maize rotation in the North China Plain. Agricultural Water Management 97, 1139–1145.

Teixeira, A.H.d.C., Bastiaanssen, W.G.M., Moura, M.S.B., Soares, J.M., Ahmad, M.D., Bos, M.G., 2008. Energy and water balance measurements for water productivity analysis in irrigated mango trees, Northeast Brazil. Agricultural and Forest Meteorology 148, 1524–1537.

Twine, T.E., Kustas, W., Norman, J., Cook, D., Houser, P., Meyers, T., Prueger, J., Starks, P., Wesely, M., 2000. Correcting eddy-covariance flux underestimates over a grassland. Agricultural and Forest Meteorology 103, 279–300.

Vandegehuchte, M.W., Braham, M., Lemeur, R., Steppe, K., 2012. The importance of sap flow measurements to estimate actual water use of Meski olive trees under different irrigation regimes in Tunisia. Irrigation and Drainage, http://dx.doi.org/10.1002/ird.1670.

Wang, J., Yu, Q., Li, J., Li, L.-H., Li, X.-G., Yu, G.-R., Sun, X.-M., 2006. Simulation of diurnal variations of $CO_2$, water and heat fluxes over winter wheat with a model coupled photosynthesis and transpiration. Agricultural and Forest Meteorology 137, 194–219.

Webb, E.K., Pearman, G.I., Leuning, R., 1980. Correction of flux measurements for density effects due to heat and water vapour transfer. Quarterly Journal of the Royal Meteorological Society 106, 85–100.

Wilczak, J.M., Oncley, S.P., Stage, S.A., 2001. Sonic anemometer tilt correction algorithms. Boundary-Layer Meteorology 99, 127–150.

Yang, Y., Watanabe, M., Zhang, X., Zhang, J., Wang, Q., Hayashi, S., 2006. Optimizing irrigation management for wheat to reduce groundwater depletion in the piedmont region of the Taihang Mountains in the North China Plain. Agricultural Water Management 82, 25–44.

Yu, G.R., Wen, X.F., Sun, X.M., Tanner, B.D., Lee, X., Chen, J.Y., 2006. Overview of ChinaFLUX and evaluation of its eddy covariance measurement. Agricultural and Forest Meteorology 137, 125–137.

Yunusa, I.A.M., Walker, R.R., Lu, P., 2004. Evapotranspiration components from energy balance, sapflow and microlysimetry techniques for an irrigated vineyard in inland Australia. Agricultural and Forest Meteorology 127, 93–107.

Zhang, B.Z., Kang, S.Z., Zhang, L., Du, T.S., Li, S.E., Yang, X.Y., 2007. Estimation of seasonal crop water consumption in a vineyard using Bowen ratio-energy balance method. Hydrological Processes 21, 3635–3641.

Zhang, Y., Kang, S., Ward, E.J., Ding, R., Zhang, X., Zheng, R., 2011a. Evapotranspiration components determined by sap flow and microlysimetry techniques of a vineyard in northwest China: dynamics and influential factors. Agricultural Water Management 98, 1207–1214.

Zhang, Y., Shen, Y., Sun, H., Gates, J.B., 2011b. Evapotranspiration and its partitioning in an irrigated winter wheat field: a combined isotopic and micrometeorologic approach. Journal of Hydrology 408, 203–211.

Zhang, Y., Shen, Y., Yu, Q., Liu, C., Kondoh, A., Tang, C., Sun, H., Jia, J., 2002. Variation of fluxes of water vapor, sensible heat and carbon dioxide above winter wheat and maize canopies. Journal of Geographical Science 12, 295–300.

Zhu, Z., Sun, X., Wen, X., Zhou, Y., Tian, J., Yuan, G., 2006. Study on the processing method of nighttime $CO_2$ eddy covariance flux data in ChinaFLUX. Science in China Series D 49, 36–46.